Metabolism of cholesterol and progesterone is differentially regulated in primary trophoblastic subtypes and might be disturbed in recurrent miscarriages[S]

Sigrid Vondra,[1,*] Victoria Kunihs,[1,*] Tanja Eberhart,[†] Karin Eigner,[†] Raimund Bauer,[†] Peter Haslinger,[*] Sandra Haider,[*] Karin Windsperger,[*] Günter Klambauer,[§] Birgit Schütz,[**] Mario Mikula,[**] Xiaowei Zhu,[††,§§] Alexander E. Urban,[††,§§] Roberta L. Hannibal,[2,§§] Julie Baker,[§§] Martin Knöfler,[*] Herbert Stangl,[†] Jürgen Pollheimer,[3,*] and Clemens Röhrl[3,†,*]**

Department of Obstetrics and Gynecology, Reproductive Biology Unit,[*] and Departments of Medical Chemistry[†] and Medical Genetics,[**] Center for Pathobiochemistry and Genetics, Medical University of Vienna, Vienna, Austria; Institute of Machine Learning,[§] Johannes Kepler University Linz, Linz, Austria; Departments of Psychiatry[††] and Genetics,[§§] Stanford University School of Medicine, Stanford, CA; and University of Applied Sciences Upper Austria,[***] Wels, Austria

ORCID IDs: 0000-0002-3621-5594 (T.E.); 0000-0002-1192-0748 (C.R.)

Abstract **During pregnancy, extravillous trophoblasts (EVTs) invade the maternal decidua and remodel the local vasculature to establish blood supply for the growing fetus. Compromised EVT function has been linked to aberrant pregnancy associated with maternal and fetal morbidity and mortality. However, metabolic features of this invasive trophoblast subtype are largely unknown. Using primary human trophoblasts isolated from first trimester placental tissues, we show that cellular cholesterol homeostasis is differentially regulated in EVTs compared with villous cytotrophoblasts. Utilizing RNA-sequencing, gene set-enrichment analysis, and functional validation, we provide evidence that EVTs display increased levels of free and esterified cholesterol. Accordingly, EVTs are characterized by increased expression of the HDL-receptor, scavenger receptor class B type I, and reduced expression of the LXR and its target genes. We further reveal that EVTs express elevated levels of hydroxy-delta-5-steroid dehydrogenase 3 beta- and steroid delta-isomerase 1 (HSD3B1) (a rate-limiting enzyme in progesterone synthesis) and are capable of secreting progesterone. Increasing cholesterol export by LXR activation reduced progesterone secretion in an ABCA1-dependent manner. Importantly, HSD3B1 expression was decreased in EVTs of idiopathic recurrent spontaneous abortions, pointing toward compromised progesterone metabolism in EVTs of early miscarriages.[JLR] Here, we provide insights into the regulation of cholesterol and progesterone metabolism in trophoblastic subtypes and its putative relevance in human miscarriage.**—Vondra, S., V. Kunihs, T. Eberhart, K. Eigner, R. Bauer, P. Haslinger, S. Haider, K. Windsperger, G. Klambauer, B. Schütz, M. Mikula, X. Zhu, A. E. Urban, R. L. Hannibal, J. Baker, M. Knöfler, H. Stangl, J. Pollheimer, and C. Röhrl. **Metabolism of cholesterol and progesterone is differentially regulated in primary trophoblastic subtypes and might be disturbed in recurrent miscarriages.** ***J. Lipid Res.*** **2019.** 60: **1922–1934**.

Supplementary key words placenta • adenosine 5′-triphosphate binding cassette transporter A1 • nuclear receptor/liver X receptor • trophoblast • HSD3B1 • scavenger receptor class B type I • early miscarriage • recurrent spontaneous abortion

Successful pregnancy relies on correct placental morphogenesis and the formation of specialized trophoblast cell types during the first weeks of gestation. Trophoblast progenitor cells emerge from the embryonic trophectoderm

This study was supported by Austrian Science Fund Grants P25763-B13 (to C.R.) and P31470-B30 (to M.K.) and Austrian National Bank Grant 17613 (Jubiläumsfonds, to J.P.). A.E.U. receives support as a Tashia and John Morgridge Faculty Scholar, Stanford Child Health Research Institute. The authors declare that they have no conflicts of interest with the contents of the article.

Manuscript received 22 February 2019 and in revised form 12 August 2019.

Published, JLR Papers in Press, September 17, 2019
DOI https://doi.org/10.1194/jlr.P093427

Abbreviations: CK7, cytokeratin 7; CTB, cytotrophoblast; EGFR, epidermal growth factor receptor; EVT, extravillous trophoblast; GO, gene ontology; GSEA, gene set-enrichment analysis; HLA, human leukocyte antigen; HMGCR, HMG-CoA reductase; HSD3B1, hydroxy-delta-5-steroid dehydrogenase 3 beta- and steroid delta-isomerase 1; ITGA, integrin subunit alpha; LDLR, LDL-receptor; LRP1, LDL-receptor-related protein 1; RNA-seq, RNA sequencing; RSA, recurrent spontaneous abortion; SA, spontaneous abortion; SR-BI, scavenger receptor class B type I; STB, syncytiotrophoblast; vCTB, villous cytotrophoblast.

The RNA sequencing data in this publication have been deposited in NCBI's Gene Expression Omnibus (Vondra et al., 2019) and are accessible through GEO Series accession number GSE126530 (https://www.ncbi.nlm.nih.gov/geo/query/acc.cgi?acc=GSE126530).

[1] S. Vondra and V. Kunihs contributed equally to this work.

[2] Present address of R. L. Hannibal: Microbiology Department, Second Genome, South San Francisco, CA.

[3] To whom correspondence should be addressed.
e-mail: clemens.roehrl@fh-wels.at (C.R.);
juergen.pollheimer@meduniwien.ac.at (J.P.)

[S] The online version of this article (available at http://www.jlr.org) contains a supplement.

and reside at the basement membrane of placental villi. These progenitor cells give rise to distinct epithelial cell types: Villous cytotrophoblasts (vCTBs) fuse to form multinucleated syncytiotrophoblasts (STBs), which cover placental floating villi and are mainly responsible for transport processes and hormone production. In anchoring villi attached to the uterine epithelium, vCTBs form proliferative cell columns. At their distal end, cell-column trophoblasts develop a highly invasive epithelial to mesenchymal transition-associated phenotype and migrate into the receptive maternal endometrium, termed decidua (1). Cytotrophoblasts (CTBs) that detach from the cell columns at their distal anchoring site and invade the maternal decidual stroma are commonly termed extravillous trophoblasts (EVTs) (2). This particular migratory and invasive, but no longer proliferative, trophoblastic subtype is crucial for the attachment of placental villi and the control of vascular remodeling of maternal spiral arteries to initiate and sustain blood flow to the growing fetus (3–5). Moreover, EVTs invade decidual veins and lymphatics (6), plug spiral arteries early in pregnancy to prevent oxidative placental damage (7), control maternal immune tolerance (8), exert defense against pathogens (9), and secrete pregnancy-specific factors into the maternal circulation (10). Faulty EVT function jeopardizes these functions causing considerable immediate and chronic health risks for both mother and child. For instance, insufficient spiral artery remodeling is a hallmark of preeclampsia (11), characterized by the de novo development of high blood pressure, nondependent edema, and proteinuria. Preeclampsia represents a leading cause of fetal and maternal morbidity and mortality, which affects 3–8% of pregnancies (12). Furthermore, compromised EVT function has also been associated with the occurrence of spontaneous abortions (SAs) and intrauterine growth restriction (6, 7).

Lipids are required by cells as energy sources, structural components, and precursors of paracrine and endocrine signaling molecules. Among the different lipid classes, cholesterol possesses particular properties: It is an essential structural component of cell membranes and a precursor of steroid hormones and bile acids. Cells gain cholesterol either by uptake from extracellular acceptors, such as lipoproteins, or by endogenous de novo synthesis from acetate. In contrast to fatty acids, cholesterol cannot be catabolized, and therefore the disposal of cholesterol from cells requires efflux to extracellular acceptors (13).

Proper growth of the human embryo requires adequate nutrient supply, especially the supply with lipids. Thus, lipid metabolism in the mature placenta as well as lipid transfer across the placenta have been the subject of extensive research (14, 15). However, knowledge on the metabolism of trophoblasts in the early stages of human placental development is sparse. On the one hand, this is due to the fact that animal models, such as the mouse, insufficiently reflect human placental development (16): Invasion of trophoblasts into the decidua is much more pronounced in humans than in animals because human embryos require abundant nutrients for the rapidly developing human brain (17). On the other hand, research on formation of the placenta is hindered due to the limited availability of primary human placental material from early pregnancy.

By using various first trimester primary human trophoblast models, we have previously shown that EVTs undergo genome amplification and cellular senescence accompanied by accumulation of glycogen and fatty acids (18). Here, we characterize cholesterol metabolism in primary human EVTs and vCTBs and attribute a functional role to cholesterol transporters in the regulation of progesterone secretion in EVTs. Furthermore, we describe differential expression of hydroxy-delta-5-steroid dehydrogenase 3 beta- and steroid delta-isomerase 1 (HSD3B1), a key enzyme in progesterone synthesis, in trophoblasts of patients with idiopathic recurrent SAs (RSAs), linking cholesterol metabolism in EVTs to human pregnancy disorders.

MATERIALS AND METHODS

Ethical considerations

All experiments and analyses were conducted in accordance with the Declaration of Helsinki as well as Austrian laws and guidelines. Isolation of primary trophoblasts from first trimester human placenta and the usage of tissue samples from subjects with idiopathic RSAs were approved by the Ethics Committee of the Medical University of Vienna (#084/2013 and #1910/2015). Ethical approvals are annually renewed. Informed consent was obtained from all subjects.

Isolation of primary human trophoblasts and separation of vCTBs and EVTs

First trimester placentae between the 6th and 12th week of gestation were derived from women undergoing elective termination of pregnancy for nonmedical reasons. Primary trophoblastic subtypes were isolated from three to six placentae per isolation according to a recently published protocol (19). Briefly, placentae were washed in ice-cold PBS and kept overnight in DMEM/Ham's F-12 medium supplemented with 0.05 mg/ml gentamicin, 100 U/ml PenStrep, and 2.5 μg/ml fungizone (all from Invitrogen, Carlsbad, CA). Villous tips were scraped with a scalpel blade and digested in 0.125% trypsin (Invitrogen) and 12.5 mg/ml DNase I (Sigma-Aldrich, St. Louis, MO) in HBSS-Mg/Ca-free medium (Sigma-Aldrich) at 37°C for 30 min without agitation. Subsequently, cells were filtered through a 100 μm cell strainer (Falcon). Cell column trophoblasts and STBs were removed by a second digestion step of the remaining tissue using 0.25% trypsin and 12.5 mg/ml DNase I for 30 min at 37°C and processed as described above. The digestion solutions were then layered on top of a Percoll gradient (10–70%; Pharmacia, Uppsala, Sweden) and centrifuged at 1,175 *g* at 4°C for 24 min without braking at the end of the run. Cells between 35% and 50% of the Percoll layer were collected. If necessary, red blood cells were lysed by incubating cells in a buffer containing 155 mM NH_4Cl, 10 mM $KHCO_3$, and 0.1 mM EDTA (pH 7.3) for 5 min. Subsequently, the cell suspension was plated in culture medium (phenol red-free DMEM/F-12 supplemented with 10% FBS, 0.05 mg/ml gentamicin, and 0.5 μg/ml fungizone) for 45 min in order to remove adherent stromal cells. Nonadherent trophoblastic cells were then collected and separated into human leukocyte antigen (HLA)G+ EVTs by magnetic-activated cell sorting using HLAG-PE antibodies, which were labeled with anti-PE micro-beads (Miltenyi Biotec, Bergisch Gladbach, Germany). The remaining HLAG-negative trophoblastic cells represent epidermal growth factor receptor (EGFR)+ vCTBs (19).

For in vitro generation of STBs by spontaneous fusion of vCTBs, vCTBs were seeded onto fibronectin-coated dishes at a density of 3.25×10^5 cells per square centimeter. EVTs and STB cultures were routinely analyzed by light microscopy and tested for expression of phenotypical markers (supplemental Fig. S1).

For RNA-sequencing (RNA-seq) analysis, EGFR+ and HLAG+ trophoblasts were separated from first trimester placentae from week 10 to week 12 of gestation by magnetic bead sorting using EGFR-PE and HLAG-PE antibodies (supplemental Table S1). In total, four sets of EGFR+ and HLAG+ trophoblasts isolated from single placentae were subjected to RNA isolation and subsequent RNA-seq analysis.

Cells were directly processed for RNA-seq, gas chromatography, quantitative (q)RT-PCR, or immunoblotting without cultivation. For measuring progesterone secretion, EVTs were cultivated as described below.

RNA-seq

RNA was extracted using the AllPrep DNA/RNA/miRNA Universal kit (Qiagen). Total RNA was depleted from rRNA using the NEBNext rRNA depletion kit (NEB, Ipswich, MA). Libraries were prepared from rRNA-depleted total RNA using the NEBNext Ultra Directional RNA Library Prep kit with the NEBNext High-Fidelity 2X PCR Master Mix (both from NEB). The libraries were analyzed on a NextSeq 500 sequencer (Illumina, San Diego, CA) with an average of 10 million reads per library using paired-end sequencing (2×150 bp).

RNA-seq data quality was evaluated using FastQC v0.11.4 and the Illumina sequencing adaptor sequences were trimmed using Cutadapt v1.8.1. The trimmed reads were mapped to the human reference genome (NCBI v37) with TopHat v2.0.14 (20), which is a fast splice junction mapper that aligns RNA-seq reads to mammalian-sized genomes using the ultra-high-throughput short read aligner, Bowtie v2.1.0 (21). The alignment output was submitted to Cufflinks v2.1.1 to assemble transcript isoforms and to estimate expression abundances on transcript and gene levels (22). Transcript abundance was quantified in fragments per kilobase of exon per million fragments mapped (FPKM) values.

RNA-seq data have been deposited in NCBI's Gene Expression Omnibus and are accessible through GEO Series accession number GSE126530 (https://www.ncbi.nlm.nih.gov/geo/query/acc.cgi?acc=GSE126530).

Bioinformatics analysis of RNA-seq data

Differentially regulated genes from RNA-seq analysis were classified as genes either upregulated $\geq$1.4-fold or downregulated $\leq$0.7-fold at a *P*-value of $P \leq 0.05$. Classification of differentially regulated genes according to gene ontology (GO) annotations was performed using WebGestalt (version 2019) by GO slim analysis (23). Gene set-enrichment analysis (GSEA) of ranked genes was done using the same software and the hallmark gene set collection as database (24). Overrepresentation enrichment analysis of differentially regulated genes in cholesterol-related pathways was performed using WebGestalt (version 2013) by Pathway Commons analysis and transcription factor target analysis (25). The following parameters were applied: significance level, 0.05; statistics test, hypergeometric; MTC, BH; minimum, 2.

Gas chromatography

The content of free cholesterol and cholesteryl esters from purified vCTBs and EVTs was analyzed by gas chromatography (26). Lipids were isolated from cell pellets by standard Folch extraction. An aliquot of the pellet was used for cell protein determination by the Bradford assay. Lipids were separated using a GC-2010 gas chromatograph (Shimadzu, Kyoto, Japan) equipped with a programmed temperature vaporizer injector and a ZB-5HT capillary column (15 m × 0.32 mm × 0.1 μm; Phenomenex, Aschaffenburg, Germany). Tridecanoyl glycerol and cholesteryl myristate (Sigma-Aldrich) were used as standards for free and esterified cholesterol, respectively. Chromatograms were analyzed using GC Solutions 2.3 (Shimadzu) and values were normalized to cell protein.

qRT-PCR and Western blot

RNA was isolated from purified vCTBs and EVTs and reverse transcription was performed according to standard methods. Gene expression was quantified by qPCR using specific TaqMan-probes (see supplemental Table S2 for details). Results were normalized to GAPDH expression.

For Western blot analysis, cells were lysed in 0.03 mol/liter Tris-HCl containing 1% sodium dodecyl sulfate, 5% glycerol, 2.3% 2-mercaptoethanol, and 0.02% bromophenol blue. Protein extracts were separated by SDS-PAGE, blotted onto methanol-activated polyvinylidene difluoride membranes (GE Healthcare, Buckinghamshire, UK), and incubated overnight at 4°C with primary antibodies as listed in supplemental Table S1. Finally, blots were incubated for 1 h at room temperature with HRP-conjugated secondary antibodies. Signals were developed using Western-Bright Quantum HRP substrate (Advansta) and visualized with a ChemiDoc imaging system (Bio-Rad). Blots were semi-quantitatively analyzed by densitometry using ImageJ 1.47v (National Institutes of Health).

Immunofluorescence of placental tissue sections

First trimester placental tissues were fixed with 7.5% (w/v) formaldehyde and embedded in paraffin (Merck, Darmstadt, Germany). Serial sections (2 μm) were cut using a microtome (HM355; Microm) and deparaffinized, and antigens were retrieved in PT Module Buffer 1 (citrate buffer, pH 6; Thermo Fisher Scientific) by KOS MicrowaveStation (Milestone SRL, Sorisole, Italy). Subsequently, sections were blocked in blocking buffer (1× PBS containing 5% FBS and 0.3% Triton™ X-100) and incubated with primary antibodies listed in supplemental Table S1 overnight at 4°C. Afterwards, slides were washed three times and incubated for 1 h with secondary antibodies (2 μg/ml). Nuclei were stained with 1 μg/ml DAPI. Images were acquired on a fluorescence microscope (Olympus BX50) and digitally photographed (F-View soft imaging system digital camera, Cell^P software; Olympus, Hamburg, Germany). To make immunofluorescence double stainings visible, corresponding colors were added to the original black-and-white images and overlays were constructed using Adobe Photoshop software. Intensity strength was analyzed using ImageJ 1.47v (National Institutes of Health).

siRNA-mediated gene silencing

Isolated EVTs were transfected with a pool of different siRNAs targeting ABCA1 or a nontargeting control pool (L-004128-00-0005 and D-001810-10-20 ON-TARGETplus SMARTpools; Dharmacon-Thermo Fisher Scientific; final siRNA concentration, 50 nM) using Lipofectamine RNAiMAX transfection reagent (Life Technologies) according to the manufacturer's instructions. After 48 h, transfected EVTs were treated with LXR agonists for another 24 h and either lysed and subjected to Western blot analysis or used to measure progesterone secretion as described below.

Progesterone secretion

For comparative analyses between EVTs and STBs, cells were seeded at the same cell density and cultivated for 72 h in phenol red-free media. Progesterone secretion was determined during the last 24 h of cultivation. For experiments to deplete cells from cholesterol or to interfere with cholesterol efflux, EVTs were cultivated for 48 h on fibronectin-coated wells (20 μg/ml; BD

Biosciences, Bedford, MA) in phenol red-free DMEM/F-12 supplemented with 10% FBS, 0.05 mg/ml gentamicin, and 0.5 μg/ml fungizone (Gibco). Cells were then cultivated in the presence or absence of compounds of interest for 24 h. Cholesterol depletion medium contained 10% lipoprotein-deficient serum [prepared as described (27)] instead of FBS and was supplemented with 5 μM lovastatin and 100 μM mevalonate (both from Sigma-Aldrich) (28). Treatment with TO901317 (10 μM), GW3695 (1 μM), probucol (10 μM; all from Sigma-Aldrich) or the combination treatment was performed in media containing 10% FBS. Progesterone secretion was quantified by ELISA (Enzo Life Sciences, Lausen, Switzerland). To exclude an effect of differences in cell number due to treatment, viable cells were counted at the end of each experiment. Cell number was neither affected by cholesterol depletion (*t*-test, $P = 0.640$) nor by treatment with LXR agonists, probucol, or the combination of both (ANOVA, $P = 0.971$ for TO901317; $P = 0.837$ for GW3695) nor by siRNA-mediated silencing in combination with LXR activation (ANOVA, $P = 0.958$).

Samples from idiopathic RSAs

Paraffin-embedded decidua basalis tissues of RSA cases (n = 23) were received from the archive of the Clinical Institute of Pathology, Medical University of Vienna. Therefore, a computer-based search was conducted to identify women with the diagnosis of idiopathic RSA between the years 2006 and 2016 and whose abortive material was histologically examined at our Clinical Institute, as recently published (6). Diagnosis of idiopathic RSA was defined as miscarriages of three or more consecutive pregnancies before 20 weeks of gestation of unexplained origin and based on ultrasound examination. Women were excluded if one of the following screening investigations revealed a possible contributing factor for their pregnancy losses: antiphospholipid syndrome, thrombophilia (activated protein C resistance, Leiden factor V mutation, prothrombin gene mutation, protein C and S deficiency, antithrombin III deficiency), uterine anomaly, hormonal dysfunction (polycystic ovarian syndrome, diabetes mellitus, abnormal thyroid function, hyperprolactinemia, luteal insufficiency), folate deficiency, infections (chlamydia, toxoplasmosis, and ureoplasma), or chromosomal aberrations.

Statistics

Data are depicted as mean ± SD. Two-sided *t*-tests were applied to compare two experimental groups (Figs. 1A; 2; 5A, B). One sample *t*-tests were used to compare data to normalized controls (Figs. 3A, B, D; 4A). ANOVA followed by Tukey's multiple testing corrections was used to compare more than two experimental groups (Fig. 5C, D). Mann-Whitney-U-test was used to compare quantification from immunofluorescence images (Figs. 3G, 4D, 6B). Significant *P*-values are indicated as: $*P \leq 0.05$, $**P \leq 0.01$, or $***P \leq 0.001$.

RESULTS

Differential regulation of cholesterol homeostasis in vCTBs and EVTs

We aimed to characterize metabolic characteristics of human trophoblast subtypes of villous (vCTBs) and extravillous (EVTs) origins. Particularly, we were interested in putative differences in cholesterol metabolism between noninvasive proliferative vCTBs and invasive migratory EVTs. Therefore, primary human trophoblasts were isolated from healthy first trimester placental tissue derived from women undergoing elective termination of pregnancy. Trophoblasts were separated into EGFR+ (vCTBs) and HLAG+ (EVTs) trophoblasts and subjected to RNA-seq analysis. Isolated trophoblast subtypes displayed typical marker gene signatures: EVTs showed reduced expression of EGFR, integrin subunit alpha (ITGA)6, serine peptidase inhibitor Kunitz type 1 (SPINT1), and endogenous retrovirus group FRD member 1 (ERVFRD1) and highly elevated expression of HLAG, ITGA1, ITGA5, and erb-b2 receptor tyrosine kinase 2 (ERBB2) (**Fig. 1A**).

To get insights into the overall diversity of vCTBs and EVTs, differentially expressed genes were first classified according to their GO annotations. Differentially expressed genes cover the top biological process categories: "biological regulation," "metabolic process," and "response to stimulus" (Fig. 1B). Strikingly, about 70% of the altered transcripts were associated with metabolic processes. Additional classifications of these genes according to their cellular component and molecular function categories are shown in supplemental Fig. S2.

Subsequently, GSEA was performed using the collection of hallmark gene sets, representing a refined and nonredundant selection covering a multitude of founder gene sets (24). EVTs displayed a strong enrichment of gene sets related to interferon response, hypoxia, and epithelial mesenchymal transition, consistent with the migratory phenotype of this cell type (supplemental Fig. S3). Highly enriched pathways in vCTBs included gene sets related to cell cycle progression, consistent with the proliferative phenotype of these cells, as well as oxidative phosphorylation. Moreover, an enrichment of the genes sets "cholesterol homeostasis" and "fatty acid metabolism" was found in these cells (supplemental Fig. S3). Focusing on pathways relevant to cholesterol metabolism, enrichment analysis of genes differentially expressed in vCTBs and EVTs revealed that differentially regulated mRNAs show a significant over-representation in the pathways "metabolism of lipids and lipoproteins," "cholesterol biosynthesis," and "metabolism of steroid hormones" (Fig. 1C). Moreover, we found an enrichment of genes targeted by the transcription factors SREBP and LXR.

EVTs display increased cholesterol levels

In order to functionally validate and confirm the results of the GSEA, we analyzed villous EGFR+ (vCTBs) and HLAG+ (EVTs) trophoblast subtypes in terms of cholesterol content by gas chromatography. Interestingly, EVTs showed an approximately 2-fold increase in cholesterol content compared with vCTBs, being mainly a result of elevated free cholesterol levels (**Fig. 2**, supplemental Fig. S4). In addition, there was a trend toward increased cholesteryl esters in EVTs, which are esterified with fatty acids and represent the storage form of cholesterol. These results confirm the differential regulation of cholesterol metabolism in vCTB and EVT subtypes.

EVTs show altered expression of genes mediating cholesterol uptake, synthesis, and efflux

Cholesterol metabolism is predominantly regulated by uptake from extracellular donors, by endogenous de novo

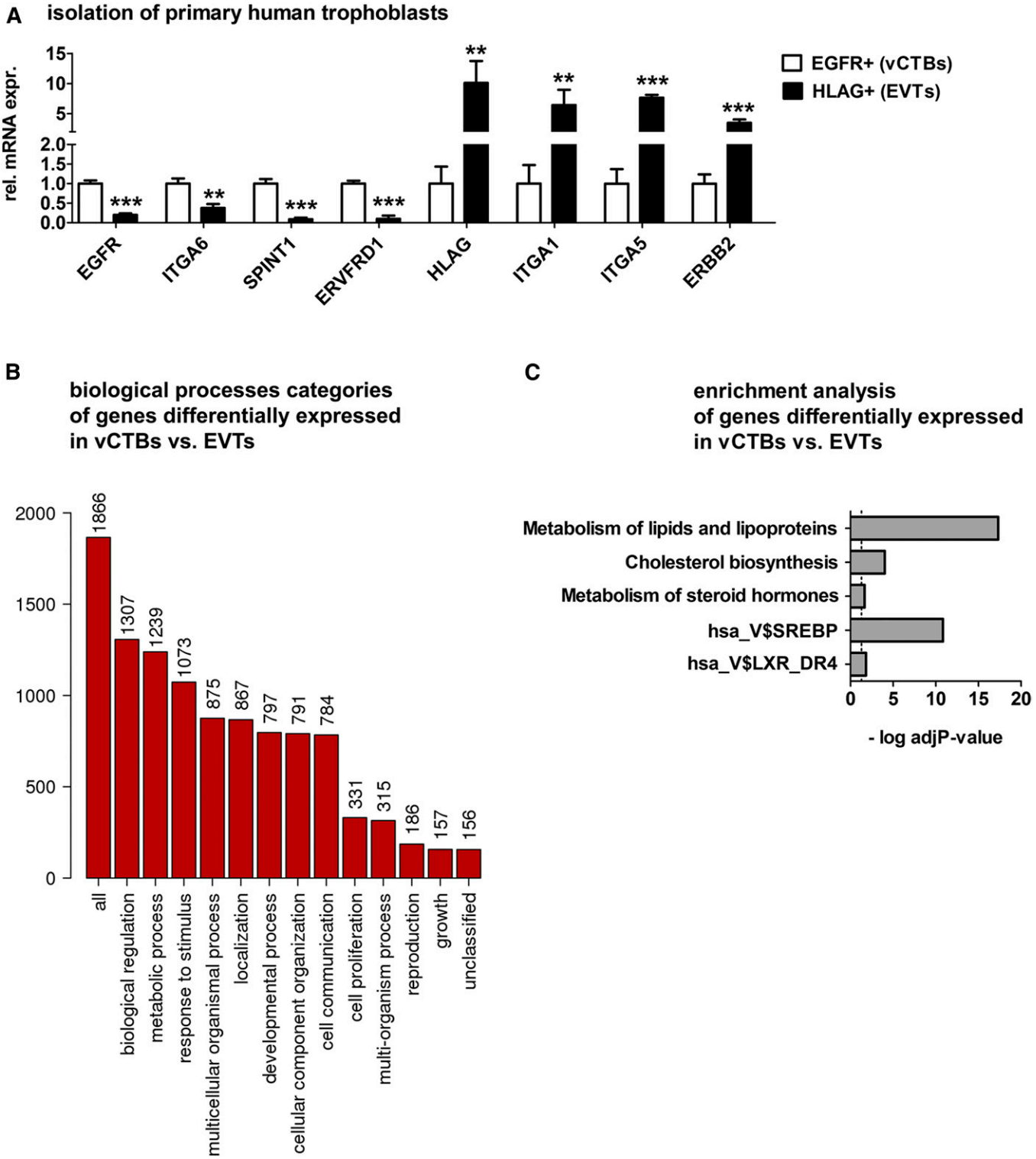

Fig. 1. Cholesterol metabolism is differentially regulated in vCTBs and EVTs. Primary human trophoblasts were isolated from first trimester placental tissue and separated into EGFR+ vCTBs and HLAG+ EVTs. RNA was isolated and analyzed by RNA-seq. A: Confirmation of the enrichment of specific trophoblast fractions (RNA-seq data from n = 4 independent trophoblast isolations; error bars represent SDs; $^{**}P \leq 0.01$, $^{***}P \leq 0.001$.) B: Genes differentially expressed between vCTBs and EVTs were analyzed according to their GO annotations and assigned to biological processes categories. The y axis represents absolute frequencies of genes in the respective category. C: Enrichment of differentially regulated genes in pathways involved in cholesterol and steroid hormone homeostasis as well as in gene sets targeted by the transcription factors SREBP and LXR. *P*-values were adjusted for multiple testing. ERVFRD1, endogenous retrovirus group FRD member 1; ERBB2, erb-b2 receptor tyrosine kinase 2; SPINT1, serine peptidase inhibitor Kunitz type 1.

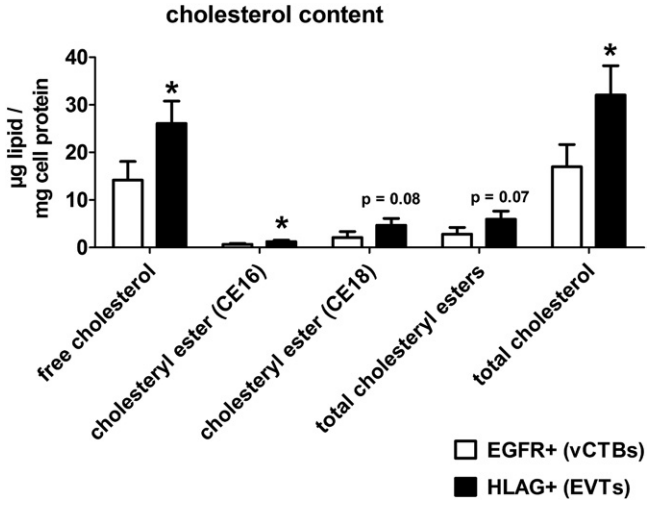

Fig. 2. EVTs display increased cholesterol content. Primary human trophoblasts were isolated from first trimester placental tissue, separated into EGFR+ vCTBs and HLAG+ EVTs and analyzed by gas chromatography. Total cholesteryl ester content is split into CE16 and CE18 (cholesterol esterified to a fatty acid containing 16 and 18 C-atoms, respectively). Total cholesterol is calculated as the sum of free cholesterol and total cholesteryl esters. Data are derived from n = 3 independent isolations. Error bars represent SDs; $*P \leq 0.05$.

synthesis, or by cholesterol efflux. Extensive qPCR analysis revealed EVT-associated decreased expression levels of the LDL-receptor (LDLR) and LDLR-related protein 1 (LRP1). The mRNA expression levels of the HDL-receptor, scavenger receptor class B type I (SR-BI), tended to be elevated in EVTs (**Fig. 3A**). Consistent with mRNA levels, protein expression of LRP1 was decreased in EVTs (Fig. 3C). In contrast, protein expression of SR-BI was increased. Furthermore, the expression level of HMG-CoA reductase (HMGCR), the rate-limiting enzyme of cholesterol biosynthesis, was decreased in EVTs (Fig. 3B, C). Moreover, expression levels of SREBP2, the transcription factor regulating numerous enzymes in the cholesterol biosynthesis pathway, were found to be reduced in EVTs (Fig. 3B). Altogether, this strongly suggests that cholesterol de novo synthesis is not increased in EVTs. Rather, reduced expression of SREBP2, HMGCR, and LDLR mRNA indicate a negative feedback loop provoked by accumulation of cellular cholesterol in EVTs.

Finally, the expression levels of LXRα and LXRβ and their target genes were analyzed. LXRα and -β are closely related nuclear receptors that respond to intracellular cholesterol levels and transcriptionally increase the expression of genes involved in cholesterol efflux, including ABCA1 (29). Expression levels of LXRα and -β as well as ABCA1 were reduced in EVTs compared with vCTBs (Fig. 3D). Similarly, the bona fide LXR target, inducible degrader of the LDLR (IDOL), was downregulated (30). Expression of ABCG1, ABCG5, or ABCG8, cholesterol export proteins that contribute to cholesterol efflux in tissues such as liver, intestine, or macrophages, was not detected in vCTBs or in EVTs according to the RNA-seq data (not shown). Reduced expression of ABCA1 in isolated EVTs was confirmed by immunoblotting (Fig. 3E) and via immunofluorescence staining of human first trimester placental tissue (Fig. 3F, G). These data suggest that increased levels of SR-BI as well as reduced expression of genes regulating cholesterol export may lead to the observed accumulation of cholesterol in EVTs.

The LXR-ABCA1 axis regulates progesterone secretion in EVTs

We next aimed to analyze progesterone secretion from cultivated primary human trophoblasts. We focused on progesterone because: *i*) cholesterol is a precursor for steroid hormone synthesis; *ii*) we found an enrichment of genes involved in the metabolism of steroid hormones (compare Fig. 1C); and *iii*) progesterone production in the placenta is critical for a successful pregnancy. Of note, the human placenta cannot further convert progesterone to other steroid hormones because it lacks expression of CYP17A1 (31).

First, the expression of key enzymes involved in progesterone synthesis from cholesterol was analyzed in vCTBs and EVTs. We did not observe alterations in the expression of cytochrome P450 family 11 subfamily A member 1 (CYP11A1) (encoding for the monooxygenase P450SCC), which catalyzes the conversion of cholesterol to pregnenolone, the first and rate-limiting step in the synthesis of steroid hormones (**Fig. 4A**). However, EVTs displayed a considerable increase in the expression of HSD3B1, which catalyzes conversion of pregnenolone to progesterone. Elevated expression of HSD3B1 was confirmed in isolated primary trophoblasts by immunoblotting (Fig. 4B) and by immunofluorescence-based analysis of human first trimester placental tissue sections (Fig. 4C, D). The latter analysis confirms that HSB3B1 is not detectable in cytokeratin 7 (CK7)+ monolayers of vCTBs (see inset 1 in Fig. 4C). In contrast, overlying CK7+ multinucleated STBs express high levels of HSD3B1 as described (32).

Given the association of high levels of cellular cholesterol with high expression of HSD3B1 in EVTs, we tested the hypothesis that cellular cholesterol levels are a direct regulator of HSD3B1 expression. However, neither depletion of cellular cholesterol levels nor activation of LXR altered the expression of HSD3B1 (supplemental Fig. S5).

Next, progesterone secretion of EVTs was analyzed in vitro. Of note, progesterone secretion of EVTs could not be compared with vCTBs because vCTBs cannot be sustained in tissue culture (19). Therefore, progesterone secretion of EVTs was compared with in vitro-generated STBs, which are the main source of progesterone production by the placenta. Indeed, EVTs secreted progesterone in amounts comparable to STBs (**Fig. 5A**), indicating that EVTs are also an abundant source of progesterone in the placenta. When EVTs were depleted from cholesterol, progesterone production was decreased, indicating that cholesterol availability limits progesterone synthesis (Fig. 5B).

Next, we tested to determine whether cholesterol efflux mediated by the LXR-ABCA1 axis is functionally involved in the regulation of progesterone production in EVTs.

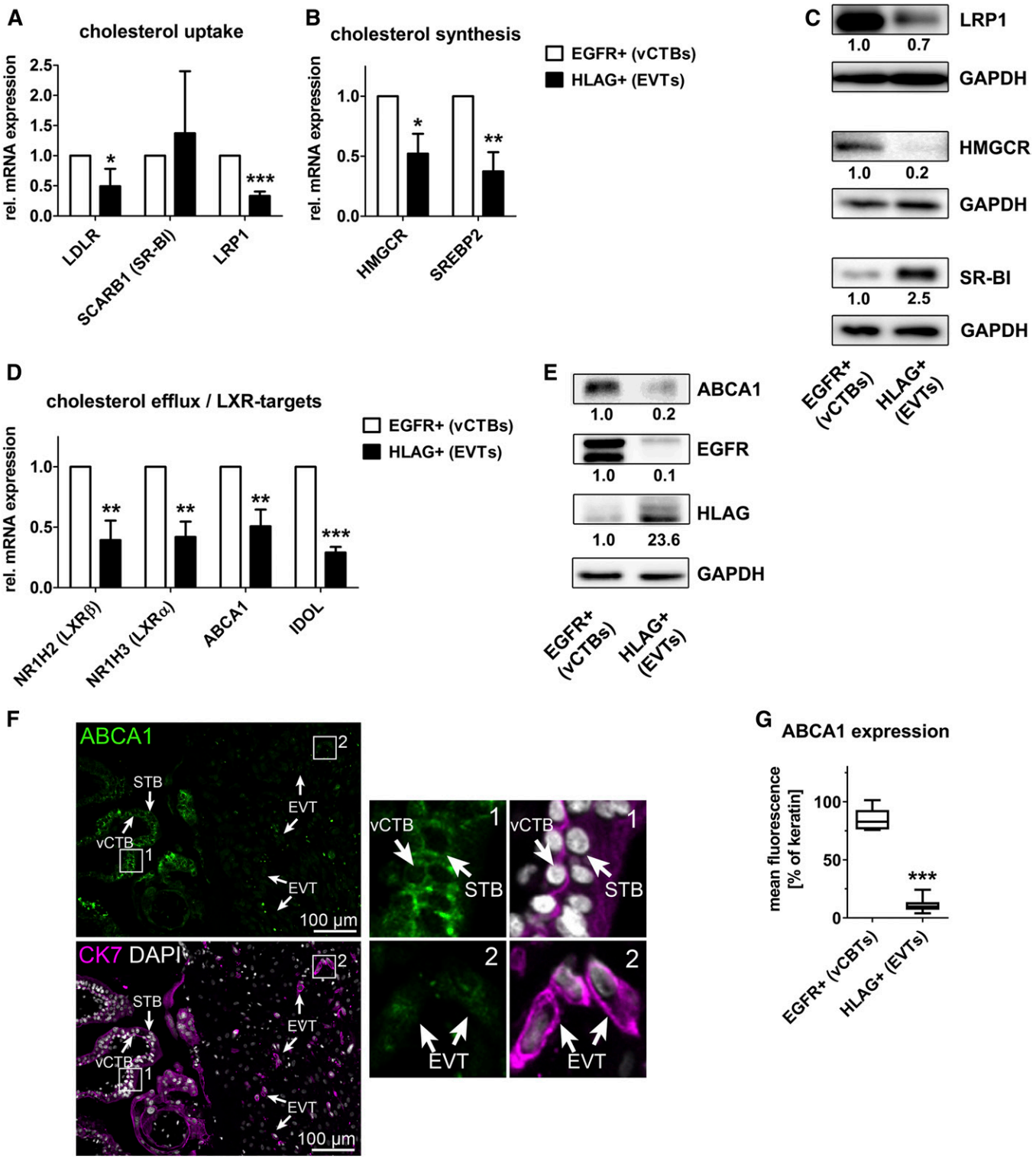

Fig. 3. Expression of genes involved in cholesterol uptake, synthesis, and export is altered in EVTs. Primary human trophoblasts were isolated from first term placental tissue, separated into EGFR+ vCTBs and HLAG+ EVTs, and analyzed by qRT-PCR (A, B, D). Data are derived from n = 4 independent isolations. Error bars represent SDs. C, E: Immunoblot analysis and quantification of n = 2 independent trophoblast isolations. F: Immunofluorescence staining of placental tissue sections (n = 5; one representative image is shown) showing ABCA1 (green) expression. CK7 (magenta) staining was used to identify trophoblasts. DAPI (gray) was used to visualize cell nuclei. G: ABCA1 staining in trophoblast subtypes was quantified and normalized to CK7 staining (quantification of 10 images derived from five different tissue samples). $*P \leq 0.05$, $**P \leq 0.01$, and $***P \leq 0.001$.

Cholesterol efflux was induced by activation of LXR by the synthetic agonist TO901317 or GW3695. This approach provoked a significant reduction in progesterone secretion (Fig. 5C). Importantly, this effect was abolished in the presence of probucol, an inhibitor of ABCA1 (33). Similarly, siRNA-mediated silencing of ABCA1 expression reverted

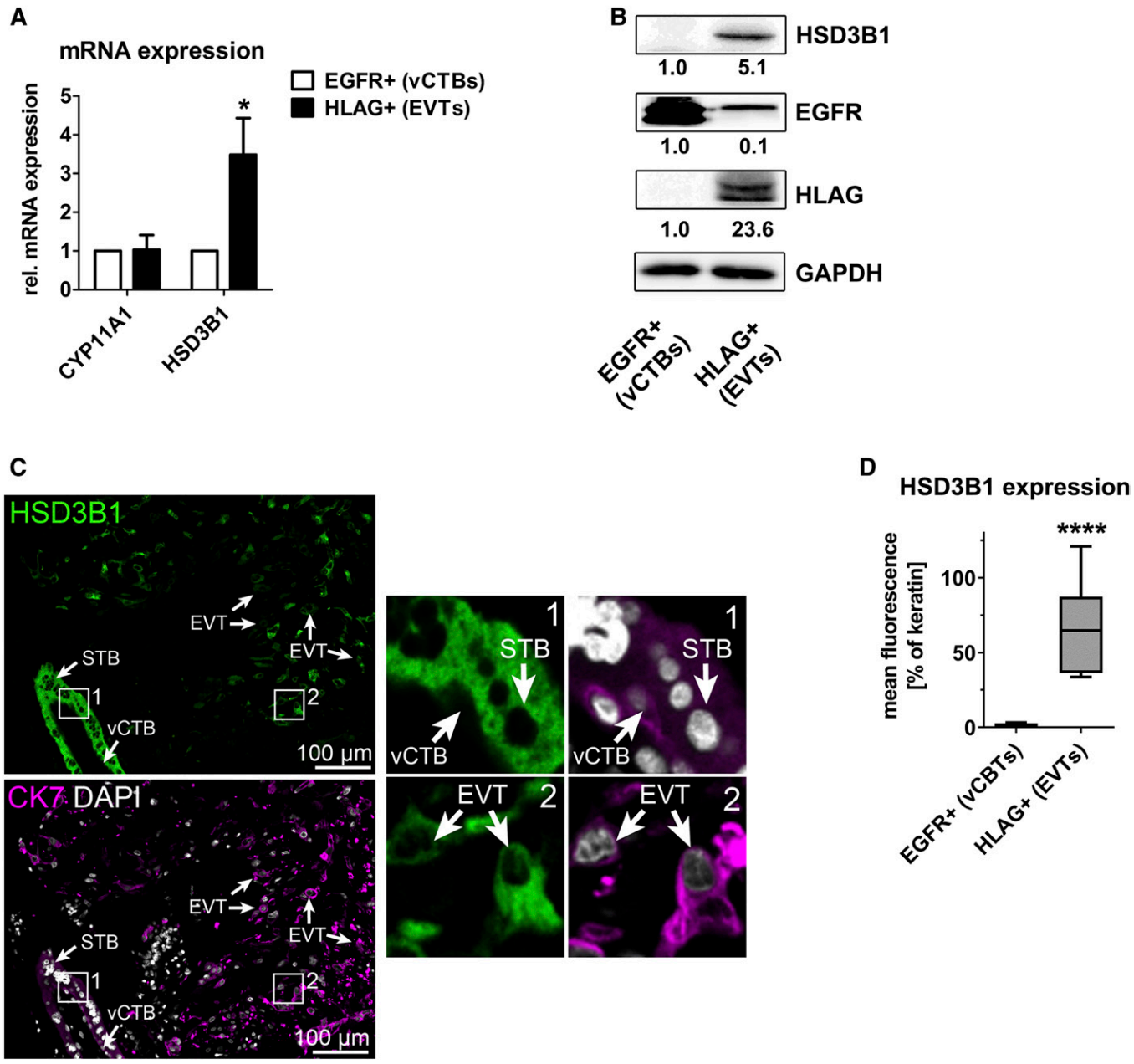

Fig. 4. Expression of HSD3B1 is increased in EVTs. Primary human trophoblasts were isolated from first trimester placental tissue, separated into EGFR+ (villous) and HLAG+ (extravillous) trophoblasts, and analyzed by qRT-PCR (A). Data are derived from n = 3 independent isolations. Error bars represent SDs. B: Immunoblot analysis and quantification of n = 2 independent trophoblast isolations. C: Immunofluorescence staining of placental tissue sections (n = 5; one representative image is shown) showing HSD3B1 (green) expression. CK7 (magenta) staining was used to identify trophoblasts. DAPI (gray) was used to visualize cell nuclei. D: HSD3B1 staining in trophoblast subtypes was quantified and normalized to CK7 staining (quantification of 10 images derived from five different tissue samples). $*P \leq 0.05$, $****P < 0.0001$.

the effect of LXR activation (Fig. 5D, E), altogether indicating that LXR regulates progesterone secretion in an ABCA1-dependent manner. Taken together our data suggest that reduced activity of LXR and ABCA1 in EVTs is accompanied by cholesterol accumulation and sustained progesterone production.

EVT-associated expression of HSD3B1 is reduced in RSAs

Finally, we aimed to clarify whether cholesterol and progesterone metabolism in EVTs is pathophysiologically relevant in early miscarriage. To this end, we analyzed a cohort of 23 cases of idiopathic RSA (6) for the expression of ABCA1 and HSD3B1. EVTs from RSA tissues did not show altered ABCA1 levels (supplemental Fig. S6). However, low expression levels of ABCA1 in EVTs per se might hinder the detection of differences between RSA patients and control subjects.

In contrast, we found a significant reduction in the expression of HSD3B1 in EVTs from patients with RSA compared with age-matched healthy controls (**Fig. 6**). It is of note that HSD3B1 expression in STBs was unchanged in RSA (Fig. 6). These data link, for the first time, an EVT-specific

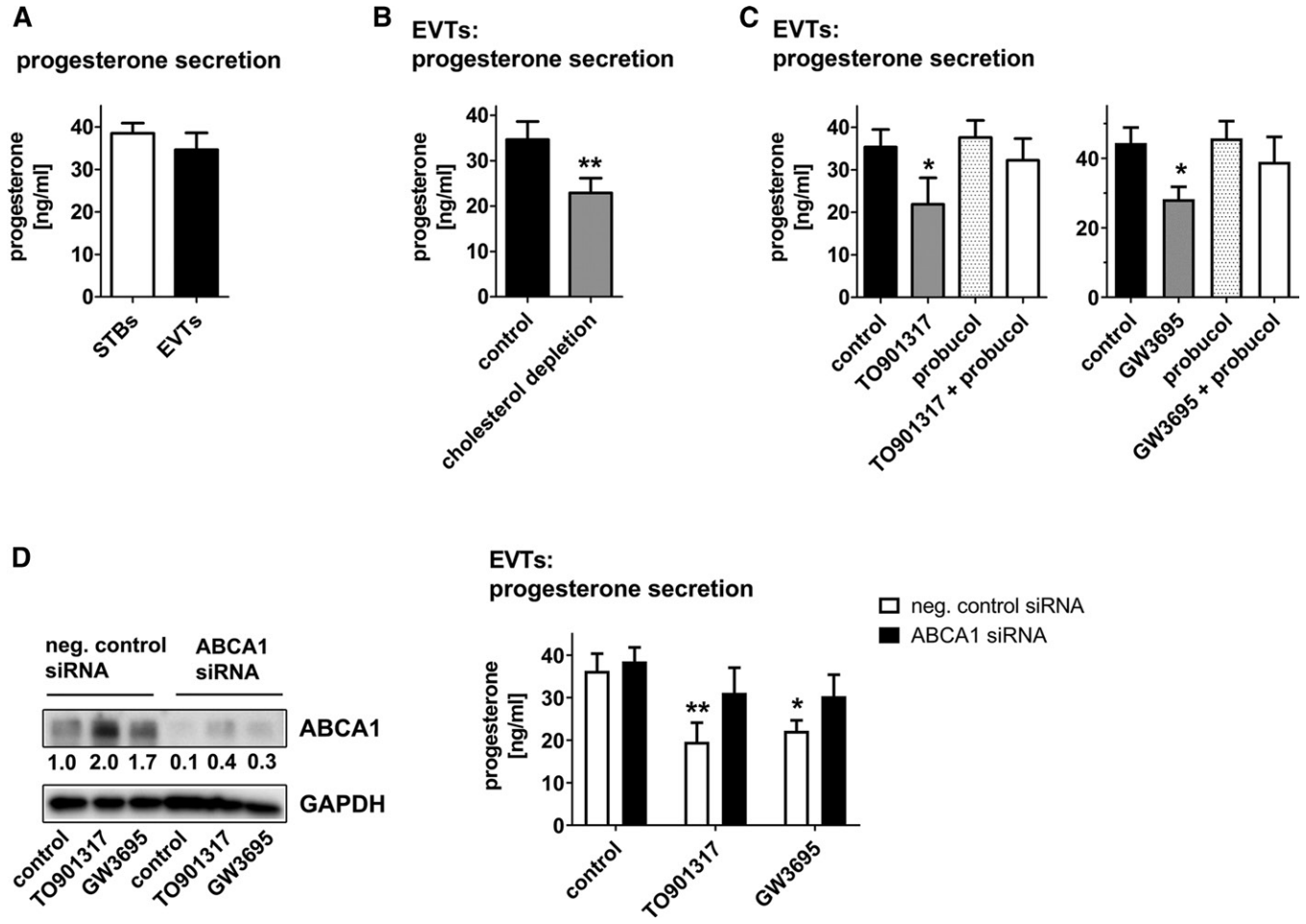

Fig. 5. The LXR-ABCA1 axis controls progesterone secretion in EVTs. EVTs were isolated from first trimester human placenta and compared with STBs (STBs) in terms of progesterone secretion into the supernatant (A). B: EVTs were cultivated either in media containing FBS or in cholesterol depletion media (see the Materials and Methods section) for 24 h. C: EVTs were cultivated in the presence or absence of the LXR-agonist TO901317 or GW3695, the ABCA1-inhibitor probucol, or in combination for 24 h. D: ABCA1 was depleted from cultured EVTs by siRNA followed by LXR-agonist treatment, and expression was analyzed by immunoblot (quantification of immunoblots of n = 2 independent trophoblast isolations are shown). E: Quantification of progesterone secretion by ELISA after siRNA knockdown and stimulation with LXR agonists. Data on progesterone secretions are derived from at least n = 3 independent experiments. Error bars represent SDs; $*P \leq 0.05$, $**P \leq 0.01$.

compromised progesterone metabolism to the occurrence of early miscarriages.

DISCUSSION

Herein, we report the first comprehensive analysis of cholesterol metabolism in primary vCTBs and EVTs from first trimester human placenta. We provide evidence that EVTs display reduced cholesterol efflux capacity accompanied by enhanced levels of cholesterol. Further, we identify cholesterol efflux via the LXR-ABCA1 axis as a regulator of progesterone production in EVTs. Finally, our data suggest deregulation of HSD3B1 in patients with idiopathic RSAs, linking aberrant progesterone metabolism in EVTs to deranged placentation.

Proper placentation is critical for pregnancy in mammals. Placenta malformation is associated with early embryonic lethality, as revealed by a phenotyping screen in 103 lethal knockout mouse models (34). Progesterone production is among the placenta's crucial functions. After about 6–8 weeks of pregnancy, the placenta takes over progesterone production from the corpus luteum, a critical phase in pregnancy (35). It is commonly accepted that STBs are responsible for progesterone secretion and insights into its regulation have largely been obtained by studying trophoblasts from term placenta. However, knowledge about the regulation of progesterone metabolism in trophoblasts derived from the critical first trimester is sparse so far: Genbacev, Schubach, and Miller (36) observed progesterone production in cultivated primary human villous explant cultures. Later on, progesterone secretion was also confirmed in primary EVT cultures (37).

Progesterone has been shown to induce vasodilation, capillary permeability, and vascular smooth muscle cell relaxation (38–40). In addition, progesterone might be important for EVTs (which are derived from the placenta and are therefore allogenic) to escape maternal immune destruction: A recent study demonstrates a progesterone-dependent

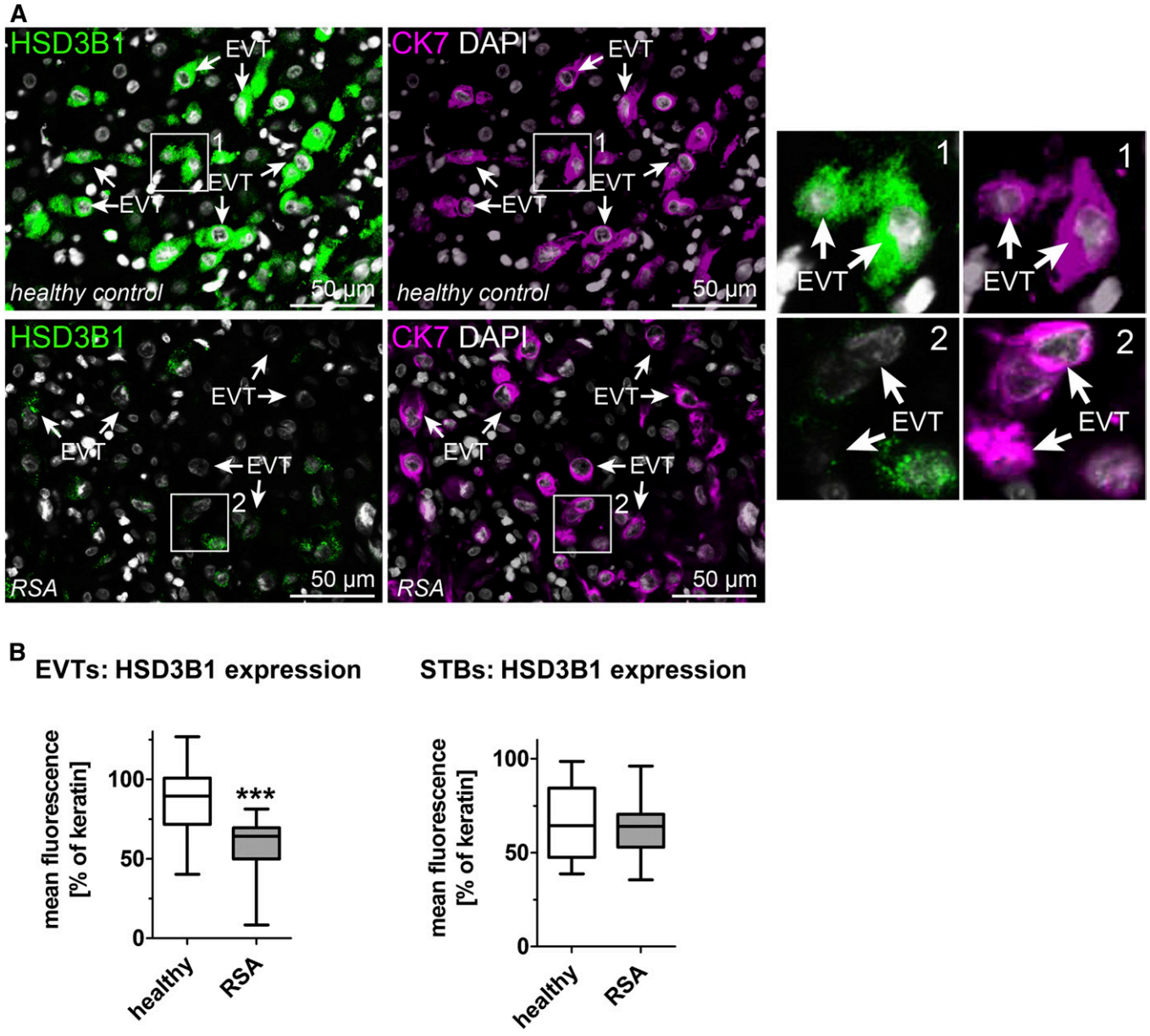

Fig. 6. HSD3B1 expression is decreased in EVTs of patients with idiopathic RSAs. A: Decidual tissue section from RSAs (n = 23) and age-matched healthy controls (n = 17) were double stained with HSD3B1 (green) and CK7 (magenta) to identify trophoblasts. DAPI (gray) was used to visualize cell nuclei. Representative images are shown. B: Quantification of HSD3B1 in CK7+ EVTs (left panel) or STBs (right panel) in RSA and age-matched healthy control tissue sections. Data were quantified from five randomized fields per tissue section. Error bars represent SDs; $***P \leq 0.001$.

role for neutrophils in the establishment of adaptive tolerance during pregnancy (41). In conclusion, local secretion of progesterone by EVTs might be important to fine-tune vascular remodeling or to escape immune destruction in the maternal decidua.

Our data show that EVTs, in comparison to vCTBs, display increased cholesterol levels, increased expression of SR-BI, which mediates cholesterol uptake of HDL, and decreased expression of ABCA1, a mediator of cholesterol efflux. Of note, the inability to culture vCTBs (19) prohibits a functional validation if either cholesterol uptake or cholesterol efflux is the underlying cause of cholesterol accumulation in EVTs compared with vCTBs, which is a limitation of the model system used.

SR-BI is a main receptor delivering cholesterol for hormone synthesis in steroidogenic tissues (42). Interestingly, SR-BI expression correlates with HSD3B1 expression in prostate cancer (43), making SR-BI a putative candidate to be responsible for cholesterol accumulation and a possible regulator of progesterone synthesis in EVTs. In our study, we focused on the role of the LXR-ABCA1 axis in progesterone production because both LXR and ABCA1 are implied to play important roles in reproduction: In mice, lack of functional ABCA1 results in severe placental malformation (44), and dysfunction of LXR is implicated in female infertility (45). ABCA1 mediates cellular efflux of cholesterol and phospholipids to extracellular acceptors such as apoA-I, the main

component of HDL, which is also present in the human endometrium (46).

LXR transcription factors are implicated in diverse cellular functions, including regulation of cholesterol efflux by ABCA1 and fatty acid synthesis in the liver as well as in extrahepatic tissues. The two LXR isoforms, LXRα and LXRβ, show distinct tissue-specific expression patterns, but display a strong overlap in the regulation of gene expression (47). Despite the fact that knowledge about the physiological role of LXR in the placenta is limited, its key functions seem to be conserved: In primary human trophoblasts from term placenta, activation of LXR likewise regulates cholesterol export and lipogenesis (48, 49).

In human first trimester placental tissues, ABCA1 is expressed in villous trophoblasts at relatively high levels (50, 51). Similarly, both LXR-isoforms are present during early placental development (52). Of note, the expression pattern of both LXR and ABCA1 shifts during pregnancy from high expression in CTBs in the first trimester to mesenchymal and endothelial cells in term placenta (53). This might aggravate the translation of findings from studies in term placenta to early events in placental development.

Studies in term placentae suggest a role of the LXR-ABCA1 axis in human pregnancy disorders: For instance, the expression of ABCA1 is downregulated in STBs under conditions of preeclampsia (54), consistent with the downregulation of LXR expression in the placenta in another study (55). LXR expression is also downregulated in the syncytium of patients with SAs and recurrent miscarriage (56). In human term trophoblasts, LXR activation by its natural agonist, 25-hydroxycholesterol, increases progesterone secretion (57). However, this sterol is a rather weak activator of LXR, possesses cytotoxic properties, and is not specific for LXR, as it interacts with other transcription factors, such as SREBPs (58, 59). In contrast, using two distinct pharmacological activators of LXR, we could clearly show that LXR is a negative regulator of progesterone secretion in primary human EVTs. Interestingly, other studies reveal that pharmacological LXR activation decreases progesterone production in luteinized granulosa cells as well as in the adrenal gland, pointing toward a general mechanism in different tissues (60, 61).

3β-HSD isoenzymes are essential enzymes in the synthesis of all classes of steroid hormones and are expressed in a tissue-specific pattern. HSD3B1 encodes for the 3β-HSD isoform expressed in the placenta (62). According to our study, HSD3B1 expression is highly elevated in EVTs compared with vCTBs. Importantly, HSD3B1 expression in EVTs was found to be reduced in patients with idiopathic RSAs, while STB-associated HSD3B1 expression was unaffected. Progesterone serum levels have been proposed to serve as predictive measures for SAs. In addition, clinical data suggest a beneficial role for progesterone supplementation to prevent recurrent miscarriage (63). The shift in progesterone production from the corpus luteum to the placenta is considered a critical window in pregnancy, particularly with respect to the occurrence of RSA (64). Given the multiple functions of progesterone in decidualization, immunoregulation, and vascularization, compromised progesterone secretion by invasive EVTs might therefore jeopardize maintenance of pregnancy.

Altogether, our data shed light on the regulation of cholesterol and progesterone metabolism in primary human trophoblasts and point toward a pathophysiologically relevant role of progesterone metabolism in early miscarriage.

REFERENCES

1. Davies, J. E., J. Pollheimer, H. E. Yong, M. I. Kokkinos, B. Kalionis, M. Knöfler, and P. Murthi. 2016. Epithelial-mesenchymal transition during extravillous trophoblast differentiation. *Cell Adh. Migr.* **10:** 310–321.
2. Knöfler, M., and J. Pollheimer. 2013. Human placental trophoblast invasion and differentiation: a particular focus on Wnt signaling. *Front. Genet.* **4:** 190.
3. Smith, S. D., C. E. Dunk, J. D. Aplin, L. K. Harris, and R. L. Jones. 2009. Evidence for immune cell involvement in decidual spiral arteriole remodeling in early human pregnancy. *Am. J. Pathol.* **174:** 1959–1971.
4. Harris, L. K., R. J. Keogh, M. Wareing, P. N. Baker, J. E. Cartwright, J. D. Aplin, and G. S. Whitley. 2006. Invasive trophoblasts stimulate vascular smooth muscle cell apoptosis by a fas ligand-dependent mechanism. *Am. J. Pathol.* **169:** 1863–1874.
5. Harris, L. K. 2010. Review: Trophoblast-vascular cell interactions in early pregnancy: how to remodel a vessel. *Placenta.* **31 (Suppl.):** S93–S98.
6. Windsperger, K., S. Dekan, S. Pils, C. Golletz, V. Kunihs, C. Fiala, G. Kristiansen, M. Knofler, and J. Pollheimer. 2017. Extravillous trophoblast invasion of venous as well as lymphatic vessels is altered in idiopathic, recurrent, spontaneous abortions. *Hum. Reprod.* **32:** 1208–1217.
7. Pijnenborg, R., L. Vercruysse, and M. Hanssens. 2006. The uterine spiral arteries in human pregnancy: facts and controversies. *Placenta.* **27:** 939–958.
8. Tilburgs, T., A. C. Crespo, A. van der Zwan, B. Rybalov, T. Raj, B. Stranger, L. Gardner, A. Moffett, and J. L. Strominger. 2015. Human HLA-G+ extravillous trophoblasts: Immune-activating cells that interact with decidual leukocytes. *Proc. Natl. Acad. Sci. USA.* **112:** 7219–7224.
9. Zeldovich, V. B., C. H. Clausen, E. Bradford, D. A. Fletcher, E. Maltepe, J. R. Robbins, and A. I. Bakardjiev. 2013. Placental syncytium forms a biophysical barrier against pathogen invasion. *PLoS Pathog.* **9:** e1003821.
10. Velicky, P., K. Windsperger, K. Petroczi, S. Pils, B. Reiter, T. Weiss, S. Vondra, R. Ristl, S. Dekan, C. Fiala, et al. 2018. Pregnancy-associated diamine oxidase originates from extravillous trophoblasts and is decreased in early-onset preeclampsia. *Sci. Rep.* **8:** 6342.
11. Brosens, I. A., W. B. Robertson, and H. G. Dixon. 1972. The role of the spiral arteries in the pathogenesis of preeclampsia. *Obstet. Gynecol. Annu.* **1:** 177–191.
12. Myatt, L. 2002. Role of placenta in preeclampsia. *Endocrine.* **19:** 103–111.
13. Ikonen, E. 2008. Cellular cholesterol trafficking and compartmentalization. *Nat. Rev. Mol. Cell Biol.* **9:** 125–138.
14. Herrera, E., and G. Desoye. 2016. Maternal and fetal lipid metabolism under normal and gestational diabetic conditions. *Horm. Mol. Biol. Clin. Investig.* **26:** 109–127.
15. Brett, K. E., Z. M. Ferraro, J. Yockell-Lelievre, A. Gruslin, and K. B. Adamo. 2014. Maternal-fetal nutrient transport in pregnancy pathologies: the role of the placenta. *Int. J. Mol. Sci.* **15:** 16153–16185.
16. Velicky, P., M. Knofler, and J. Pollheimer. 2016. Function and control of human invasive trophoblast subtypes: intrinsic vs. maternal control. *Cell Adh. Migr.* **10:** 154–162.
17. Parham, P., and A. Moffett. 2013. Variable NK cell receptors and their MHC class I ligands in immunity, reproduction and human evolution. *Nat. Rev. Immunol.* **13:** 133–144.

18. Velicky, P., G. Meinhardt, K. Plessl, S. Vondra, T. Weiss, P. Haslinger, T. Lendl, K. Aumayr, M. Mairhofer, X. Zhu, et al. 2018. Genome amplification and cellular senescence are hallmarks of human placenta development. *PLoS Genet.* **14:** e1007698.
19. Haider, S., G. Meinhardt, L. Saleh, C. Fiala, J. Pollheimer, and M. Knofler. 2016. Notch1 controls development of the extravillous trophoblast lineage in the human placenta. *Proc. Natl. Acad. Sci. USA.* **113:** E7710–E7719.
20. Trapnell, C., L. Pachter, and S. L. Salzberg. 2009. TopHat: discovering splice junctions with RNA-Seq. *Bioinformatics.* **25:** 1105–1111.
21. Langmead, B., C. Trapnell, M. Pop, and S. L. Salzberg. 2009. Ultrafast and memory-efficient alignment of short DNA sequences to the human genome. *Genome Biol.* **10:** R25.
22. Trapnell, C., B. A. Williams, G. Pertea, A. Mortazavi, G. Kwan, M. J. van Baren, S. L. Salzberg, B. J. Wold, and L. Pachter. 2010. Transcript assembly and quantification by RNA-Seq reveals unannotated transcripts and isoform switching during cell differentiation. *Nat. Biotechnol.* **28:** 511–515.
23. Liao, Y., J. Wang, E. J. Jaehnig, Z. Shi, and B. Zhang. 2019. WebGestalt 2019: gene set analysis toolkit with revamped UIs and APIs. *Nucleic Acids Res.* **47:** W199–W205.
24. Liberzon, A., C. Birger, H. Thorvaldsdottir, M. Ghandi, J. P. Mesirov, and P. Tamayo. 2015. The Molecular Signatures Database (MSigDB) hallmark gene set collection. *Cell Syst.* **1:** 417–425.
25. Wang, J., D. Duncan, Z. Shi, and B. Zhang. 2013. WEB-based gene set analysis toolkit (WebGestalt): update 2013. *Nucleic Acids Res.* **41:** W77–W83.
26. Röhrl, C., K. Eigner, K. Winter, M. Korbelius, S. Obrowsky, D. Kratky, W. J. Kovacs, and H. Stangl. 2014. Endoplasmic reticulum stress impairs cholesterol efflux and synthesis in hepatic cells. *J. Lipid Res.* **55:** 94–103.
27. Krieger, M. 1986. Isolation of somatic cell mutants with defects in the endocytosis of low-density lipoprotein. *Methods Enzymol.* **129:** 227–237.
28. Eberhart, T., K. Eigner, Y. Filik, S. Fruhwurth, H. Stangl, and C. Rohrl. 2016. The unfolded protein response is a negative regulator of scavenger receptor class B, type I (SR-BI) expression. *Biochem. Biophys. Res. Commun.* **479:** 557–562.
29. Costet, P., Y. Luo, N. Wang, and A. R. Tall. 2000. Sterol-dependent transactivation of the ABC1 promoter by the liver X receptor/retinoid X receptor. *J. Biol. Chem.* **275:** 28240–28245.
30. Zelcer, N., C. Hong, R. Boyadjian, and P. Tontonoz. 2009. LXR regulates cholesterol uptake through Idol-dependent ubiquitination of the LDL receptor. *Science.* **325:** 100–104.
31. Tuckey, R. C. 2005. Progesterone synthesis by the human placenta. *Placenta.* **26:** 273–281.
32. Mason, J. I., K. Ushijima, K. M. Doody, K. Nagai, D. Naville, J. R. Head, L. Milewich, W. E. Rainey, and M. M. Ralph. 1993. Regulation of expression of the 3 beta-hydroxysteroid dehydrogenases of human placenta and fetal adrenal. *J. Steroid Biochem. Mol. Biol.* **47:** 151–159.
33. Favari, E., I. Zanotti, F. Zimetti, N. Ronda, F. Bernini, and G. H. Rothblat. 2004. Probucol inhibits ABCA1-mediated cellular lipid efflux. *Arterioscler. Thromb. Vasc. Biol.* **24:** 2345–2350.
34. Perez-Garcia, V., E. Fineberg, R. Wilson, A. Murray, C. I. Mazzeo, C. Tudor, A. Sienerth, J. K. White, E. Tuck, E. J. Ryder, et al. 2018. Placentation defects are highly prevalent in embryonic lethal mouse mutants. *Nature.* **555:** 463–468.
35. Bhurke, A. S., I. C. Bagchi, and M. K. Bagchi. 2016. Progesterone-regulated endometrial factors controlling implantation. *Am. J. Reprod. Immunol.* **75:** 237–245.
36. Genbacev, O., S. A. Schubach, and R. K. Miller. 1992. Villous culture of first trimester human placenta–model to study extravillous trophoblast (EVT) differentiation. *Placenta.* **13:** 439–461.
37. Menkhorst, E. M., M. L. Van Sinderen, K. Rainczuk, C. Cuman, A. Winship, and E. Dimitriadis. 2017. Invasive trophoblast promote stromal fibroblast decidualization via Profilin 1 and ALOX5. *Sci. Rep.* **7:** 8690.
38. Barbagallo, M., L. J. Dominguez, G. Licata, J. Shan, L. Bing, E. Karpinski, P. K. Pang, and L. M. Resnick. 2001. Vascular effects of progesterone: role of cellular calcium regulation. *Hypertension.* **37:** 142–147.
39. Kowalik, M. K., R. Rekawiecki, and J. Kotwica. 2013. The putative roles of nuclear and membrane-bound progesterone receptors in the female reproductive tract. *Reprod. Biol.* **13:** 279–289.
40. Ancelin, M., H. Buteau-Lozano, G. Meduri, M. Osborne-Pellegrin, S. Sordello, J. Plouet, and M. Perrot-Applanat. 2002. A dynamic shift of VEGF isoforms with a transient and selective progesterone-induced expression of VEGF189 regulates angiogenesis and vascular permeability in human uterus. *Proc. Natl. Acad. Sci. USA.* **99:** 6023–6028.
41. Nadkarni, S., J. Smith, A. N. Sferruzzi-Perri, A. Ledwozyw, M. Kishore, R. Haas, C. Mauro, D. J. Williams, S. H. Farsky, F. M. Marelli-Berg, et al. 2016. Neutrophils induce proangiogenic T cells with a regulatory phenotype in pregnancy. *Proc. Natl. Acad. Sci. USA.* **113:** E8415–E8424.
42. Azhar, S., and E. Reaven. 2002. Scavenger receptor class BI and selective cholesteryl ester uptake: partners in the regulation of steroidogenesis. *Mol. Cell. Endocrinol.* **195:** 1–26.
43. Schörghofer, D., K. Kinslechner, A. Preitschopf, B. Schutz, C. Rohrl, M. Hengstschlager, H. Stangl, and M. Mikula. 2015. The HDL receptor SR-BI is associated with human prostate cancer progression and plays a possible role in establishing androgen independence. *Reprod. Biol. Endocrinol.* **13:** 88.
44. Christiansen-Weber, T. A., J. R. Voland, Y. Wu, K. Ngo, B. L. Roland, S. Nguyen, P. A. Peterson, and W. P. Fung-Leung. 2000. Functional loss of ABCA1 in mice causes severe placental malformation, aberrant lipid distribution, and kidney glomerulonephritis as well as high-density lipoprotein cholesterol deficiency. *Am. J. Pathol.* **157:** 1017–1029.
45. Dallel, S., I. Tauveron, F. Brugnon, S. Baron, J. M. A. Lobaccaro, and S. Maqdasy. 2018. Liver X receptors: a possible link between lipid disorders and female infertility. *Int. J. Mol. Sci.* **19:** E2177.
46. Brosens, J. J., A. Hodgetts, F. Feroze-Zaidi, J. R. Sherwin, L. Fusi, M. S. Salker, J. Higham, G. L. Rose, T. Kajihara, S. L. Young, et al. 2010. Proteomic analysis of endometrium from fertile and infertile patients suggests a role for apolipoprotein A-I in embryo implantation failure and endometriosis. *Mol. Hum. Reprod.* **16:** 273–285.
47. Wang, B., and P. Tontonoz. 2018. Liver X receptors in lipid signalling and membrane homeostasis. *Nat. Rev. Endocrinol.* **14:** 452–463.
48. Weedon-Fekjaer, M. S., K. T. Dalen, K. Solaas, A. C. Staff, A. K. Duttaroy, and H. I. Nebb. 2010. Activation of LXR increases acyl-CoA synthetase activity through direct regulation of ACSL3 in human placental trophoblast cells. *J. Lipid Res.* **51:** 1886–1896.
49. Aye, I. L., B. J. Waddell, P. J. Mark, and J. A. Keelan. 2010. Placental ABCA1 and ABCG1 transporters efflux cholesterol and protect trophoblasts from oxysterol induced toxicity. *Biochim. Biophys. Acta.* **1801:** 1013–1024.
50. Nikitina, L., F. Wenger, M. Baumann, D. Surbek, M. Korner, and C. Albrecht. 2011. Expression and localization pattern of ABCA1 in diverse human placental primary cells and tissues. *Placenta.* **32:** 420–430.
51. Bhattacharjee, J., F. Ietta, E. Giacomello, N. Bechi, R. Romagnoli, A. Fava, and L. Paulesu. 2010. Expression and localization of ATP binding cassette transporter A1 (ABCA1) in first trimester and term human placenta. *Placenta.* **31:** 423–430.
52. Marceau, G., D. H. Volle, D. Gallot, D. J. Mangelsdorf, V. Sapin, and J. M. Lobaccaro. 2005. Placental expression of the nuclear receptors for oxysterols LXRalpha and LXRbeta during mouse and human development. *Anat. Rec. A Discov. Mol. Cell. Evol. Biol.* **283:** 175–181.
53. Plösch, T., A. Gellhaus, E. M. van Straten, N. Wolf, N. C. Huijkman, M. Schmidt, C. E. Dunk, F. Kuipers, and E. Winterhager. 2010. The liver X receptor (LXR) and its target gene ABCA1 are regulated upon low oxygen in human trophoblast cells: a reason for alterations in preeclampsia? *Placenta.* **31:** 910–918.
54. Baumann, M., M. Korner, X. Huang, F. Wenger, D. Surbek, and C. Albrecht. 2013. Placental ABCA1 and ABCG1 expression in gestational disease: pre-eclampsia affects ABCA1 levels in syncytiotrophoblasts. *Placenta.* **34:** 1079–1086.
55. Weedon-Fekjær, M. S., G. M. Johnsen, E. H. Anthonisen, M. Sugulle, H. I. Nebb, A. K. Duttaroy, and A. C. Staff. 2010. Expression of liver X receptors in pregnancies complicated by preeclampsia. *Placenta.* **31:** 818–824.
56. Knabl, J., A. Pestka, R. Huttenbrenner, T. Plosch, R. Ensenauer, L. Welbergen, S. Hutter, M. Gunthner-Biller, and U. Jeschke. 2013. The liver x receptor in correlation with other nuclear receptors in spontaneous and recurrent abortions. *PPAR Res.* **2013:** 575604.
57. Larkin, J. C., S. B. Sears, and Y. Sadovsky. 2014. The influence of ligand-activated LXR on primary human trophoblasts. *Placenta.* **35:** 919–924.
58. Janowski, B. A., P. J. Willy, T. R. Devi, J. R. Falck, and D. J. Mangelsdorf. 1996. An oxysterol signalling pathway mediated by the nuclear receptor LXR alpha. *Nature.* **383:** 728–731.
59. Diczfalusy, U. 2013. On the formation and possible biological role of 25-hydroxycholesterol. *Biochimie.* **95:** 455–460.

60. Nilsson, M., T. M. Stulnig, C. Y. Lin, A. L. Yeo, P. Nowotny, E. T. Liu, and K. R. Steffensen. 2007. Liver X receptors regulate adrenal steroidogenesis and hypothalamic-pituitary-adrenal feedback. *Mol. Endocrinol.* **21:** 126–137.
61. Drouineaud, V., P. Sagot, C. Garrido, E. Logette, V. Deckert, P. Gambert, C. Jimenez, B. Staels, L. Lagrost, and D. Masson. 2007. Inhibition of progesterone production in human luteinized granulosa cells treated with LXR agonists. *Mol. Hum. Reprod.* **13:** 373–379.
62. Simard, J., M. L. Ricketts, S. Gingras, P. Soucy, F. A. Feltus, and M. H. Melner. 2005. Molecular biology of the 3beta-hydroxysteroid dehydrogenase/delta5-delta4 isomerase gene family. *Endocr. Rev.* **26:** 525–582.
63. Saccone, G., C. Schoen, J. M. Franasiak, R. T. Scott, Jr., and V. Berghella. 2017. Supplementation with progestogens in the first trimester of pregnancy to prevent miscarriage in women with unexplained recurrent miscarriage: a systematic review and meta-analysis of randomized, controlled trials. *Fertil. Steril.* **107:** 430–438.e3.
64. Ewington, L. J., S. Tewary, and J. J. Brosens. 2019. New insights into the mechanisms underlying recurrent pregnancy loss. *J. Obstet. Gynaecol. Res.* . **45:** 258–265.